Catal Lett (2008) 126:301–307
DOI 10.1007/s10562-008-9614-2

Partial Oxidation of Isobutane Over Hydrothermally Synthesized Mo–V–Te–O Mixed Oxide Catalysts

Jingqi Guan · Chen Xu · Bo Liu · Ying Yang · Yanyan Ma · Qiubin Kan

Received: 20 June 2008 / Accepted: 7 August 2008 / Published online: 5 September 2008

Abstract Mo–V–O and Mo–V–Te–O catalysts were prepared by a hydrothermal synthesis route and tested for the oxidation of isobutane and isobutene. Characterization results (XRD, FT-IR, TPR, BET, and XPS) showed that the structure and property of Mo–V-based catalysts are considerably different depending on the presence of Te element and calcined temperature. Catalytic tests showed that the maximum selectivity of methacrolein (44.2%) can be achieved over a $MoV_{0.3}Te_{0.25}$-600 catalyst for the selective oxidation of isobutane. It is found that TeMo-containing phases are active and selective for the selective oxidation of isobutane to methacrolein.

Keywords Isobutane · Selective oxidation · Methacrolein · Hydrothermal synthesis · Mo–V–Te–O mixed oxide catalysts

1 Introduction

The development of highly active and selective heterogeneous oxidation catalysts is essential for the successful commercialization of new catalytic processes to produce important bulk chemicals. Direct oxidation of isobutane is an example of a highly desirable process to produce methacrolein (MAL) and methacrylic acid (MAA), important chemical intermediates for the manufacture of methyl methacrylate (MMA) [1]. The majority of MMA is produced presently through the multistep catalytic oxidation reaction of acetone with hydrogen cyanide process or catalytic oxidation of isobutene. A process based on the direct oxidation of isobutane is comparatively attractive, since isobutane is much cheaper and more abundant than isobutene, which has led to intense research worldwide [2–12].

The most promising catalyst system investigated to date for isobutane oxidation to MAL is the Mo–V–Te–O-based mixed metal oxide system reported by Guan and co-workers [9–12]. This catalyst system is originally synthesized by the dry-up method, which often leads to phase mixtures including pseudohexagonal M2 phase but without M1 phase possessing orthorhombic structure. The selectivity to MAL over the Mo–V–Te–O-based system synthesized by the dry-up method is usually not excess 40%. It has been reported that the M1 phase is more active and selective than the M2 phase in propane ammoxidation [13–16]. Therefore, investigating catalytic oxidation of isobutane over M1 phase containing catalysts should be a fascinating topic for study. In the present study, we report a hydrothermal synthesis of Mo–V-based catalysts and investigate their catalytic performance for partial oxidation of lower alkane.

2 Experimental

2.1 Catalyst Preparation

Hydrothermal conditions were used for preparing the Mo–V–Te–O complex metal oxides [17]. In a typical synthesis, in 30 mL of water heated at 80 °C, 3.60 g of MoO_3, 0.68 g of V_2O_5, 0.97 g of TeO_2, and 7.5 mmol of

J. Guan · C. Xu · B. Liu · Y. Yang · Y. Ma · Q. Kan
College of Chemistry, Jilin University, Changchun 130023, People's Republic of China

Q. Kan (✉)
Jiefang Road 2519, Changchun 130021, People's Republic of China
e-mail: catalysischina@yahoo.com.cn

oxalic acid, were added to form a slurry. The slurry was introduced into a stainless autoclave equipped with a Teflon® inner tube and then the autoclave was heated at 175 °C for 48 h. After cooling, the solid obtained was separated by filtration and washed with water several times, and dried at 110 °C for 12 h to give a black solid. The sample will be denoted as $MoV_{0.3}Te_{0.25}$, which was calcined under a flow of N_2 (50 mL/min) or air (50 mL/min) to obtain the catalyst. The calcination was performed with a heating rate of 2 °C/min. The final calcination temperature was 500 °C for 2 h or 600 °C for 2 h. The samples will be designed as $MoV_{0.3}Te_{0.25}$-*X*, where *X* indicates the final calcination temperature (500 or 600 °C).

For comparison, Mo–V–O catalysts were also prepared under similar conditions.

2.2 Catalyst Characterization

The specific surface areas of the catalysts were measured based on the adsorption isotherms of N_2 at −196 °C using the BET method (Micromeritics ASAP2010). Powder X-ray diffraction (XRD) patterns were collected using a Shimadzu XRD-6000 scanning at 4°/min with Cu*K*α radiation (40 kV, 30 mA). The infrared spectra (IR) of various samples were recorded at room temperature using a NICOLET Impact 410 spectrometer.

X-ray photoelectron spectra (XPS) were recorded on a VG ESCA LAB MK-II X-ray electron spectrometer using Al*K*α radiation (1486.6 eV, 10.1 kV). The spectra were referenced with respect to the C 1s line at 284.7 eV. The measurement error of the spectra was ±0.2 eV.

H_2-temperature programmed reduction (TPR) experiments were carried out in a flow reactor system, in which 10 mg of catalyst was charged each run into a U-shaped quartz microreactor (4 mm i.d.). After purging with Ar gas from 50 to 300 °C at a ramp rate of 10 °C/min, holding at 300 °C for 30 min, and cooling to 100 °C, the sample was reduced in a 5% H_2/Ar stream (25 mL/min). The reduction temperature was raised uniformly from 100 to 800 °C at a ramp of 10 °C/min. H_2 consumption was measured by a thermal conductivity detector (TCD).

2.3 Catalytic Tests

The reaction was performed in a stainless steel tubular fixed bed reactor (16 mm i.d., 400 mm long) under atmospheric pressure. Each catalytic test was carried out using 1.0 g of catalyst, which was granulated into particles of 20–30 mesh size and diluted with 1.0 g of SiC particles to prevent temperature gradients and hot spots in the reactor. Under our reaction conditions, the homogeneous reaction can be neglected. Carbon mass balances of ≥97% were typically observed.

The feed was controlled by a mass flow controller, and water was fed by a mini-pump. The catalytic reaction condition was as follows: molar ratio of the feed gas i-C_4H_{10}: O_2: N_2: H_2O = 1:1:2:1, i-C_4H_8: O_2: N_2: H_2O = 1:2:5:2. The products were then fed via heated lines to an on-line gas chromatography for analysis. Isobutene (*i*-$C_4^=$), methacrolein (MAL), CO_x (CO, CO_2), acetic acid (HAC) propylene ($C_3^=$), acetone, methacrylic acid (MAA), acrolein, and acrylic acid were detected as products.

3 Results and Discussion

3.1 XRD Studies

XRD patterns of the prepared catalysts are shown in Fig. 1. For the Te-free sample $MoV_{0.3}O_x$ calcined in N_2 at 500 or 600 °C, the peaks at 2θ = 13.0, 23.6, 26.1, 27.6, 33.1, 34.0, 35.7, and 39.2° can be assigned to MoO_3 [JCPDS 35-0609], whereas the peaks at 2θ = 13.0, 22.2, 26.1, and 33.1° can be attributed to Mo_4O_{11} [JCPDS 13-0142]. Moreover, the peaks at 2θ = 15.0, 25.5, 26.0, 29.8, and 33.1° can be ascribed to $(Mo_{0.3}V_{0.7})_2O_5$ [JCPDS 21-0576], while the peaks at 2θ = 14.2, 22.2, 23.6, 25.5, 26.0, 27.6, 33.1, 35.7, 39.2, and 40.0° can be related to $(V_{0.07}M_{0.93})_5O_{14}$ [JCPDS 31-1437]. In addition, orthorhombic M1 phase (2θ = 13.0, 22.2, 26.9, and 45.2°) is also detected [18].

In contrast, the XRD pattern of the Te-doping sample $MoV_{0.3}Te_{0.25}$-500 indicates the presence of MoO_3, Mo_4O_{11}, $(V_{0.07}M_{0.93})_5O_{14}$, orthorhombic M1 phase (TeM_3O_{10}, *M* = Mo and V), and a new crystalline phase $TeMo_5O_{16}$ (2θ = 22.2, 23.6, 24.6, 27.6, 28.6, 33.1, 34.0,

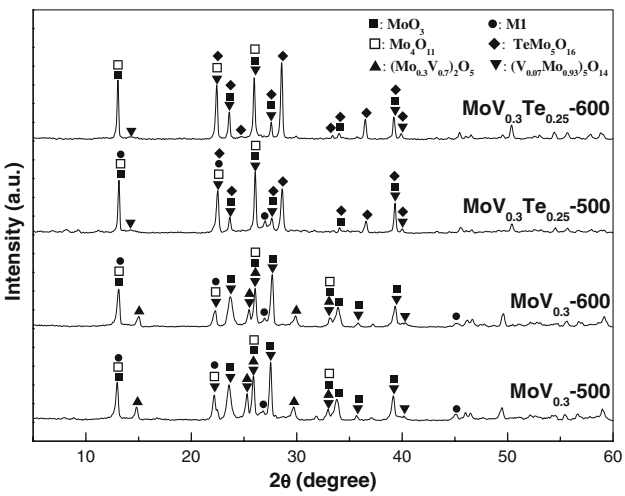

Fig. 1 XRD patterns of $MoV_{0.3}O_x$ and $MoV_{0.3}Te_{0.25}O_x$ mixed oxide catalysts calcined at 500 °C and 600 °C for 2 h in flowing N_2

36.5, 39.2, and 40.0°) [JCPDS 88-0407], while the $(Mo_{0.3}V_{0.7})_2O_5$ phase is absent. In the meanwhile, the peak at 26.9° is almost negligible in the XRD pattern for $MoV_{0.3}Te_{0.25}$-600, which suggests that the $MoV_{0.3}Te_{0.25}$-600 catalyst does not contain M1 phase.

3.2 FTIR Studies

Figure 2 displays the IR spectra of $MoV_{0.3}O_x$ and $MoV_{0.3}Te_{0.25}O_x$ mixed oxide catalysts calcined at 500 °C and 600 °C for 2 h in flowing N_2. For the Te-free sample $MoV_{0.3}O_x$, the bands at 993, 881, 820, 602, and 490 cm^{-1} can be attributed to MoO_3, whereas bands at 946 and 746 cm^{-1} are due to antisymmetric vibrations of Mo–O–V bridging bonds [19–21]. However, all of these bands can be shifted from their original positions due to incorporation of Te atoms to the system [11]. For the Te-doping sample $MoV_{0.3}Te_{0.25}O_x$, it can be seen that the bands at 993, 870, 820, and 602 cm^{-1} are associated with the presence of MoO_3, while the bands at 922, 820, and 713 cm^{-1} should be related to $TeMo_5O_{16}$ phase. It should be noted that no band due to Mo–O–V for $MoV_{0.3}Te_{0.25}O_x$ samples is found, suggesting that the $(Mo_{0.3}V_{0.7})_2O_5$ phase may be negligible in the two samples. This finding is consistent with the result from the XRD patterns.

3.3 XPS Studies

Table 1 provides the specific surface area and XPS data of the catalysts. The catalysts' specific surface areas depended on their composition and calcined temperature. In general, the specific surface area decreased with increasing the calcined temperature. The catalysts' surface composition depended on the nominated amount of each element and calcined temperature. For the Te-doping samples, the surface molybdenum content increased, while the surface vanadium content decreased with increasing the calcined temperature.

To gain deeper insight into the surface constitution and properties of these catalysts, we investigated their binding energies (Mo 3d5/2, Te 3d5/2, V 2p3/2, and O 1s). The corresponding spectra are plotted in Fig. 3, which are composed and integrated with the results listed in Table 1. The Mo 3d5/2 peak of the catalysts can be fitted mainly into two components at 231.7 and 232.8 eV, which can be related to Mo^{5+} and Mo^{6+}, respectively [11, 22]. However, the binding energy of Mo ions in a 4+ oxidation state (typical value of 230.9 eV in MoO_2) is not observed [23]. As shown in Fig. 3 and Table 1, the Mo^{5+}/Mo^{6+} surface atomic ratios increased with the calcined temperature.

The V 2p3/2 peak of catalysts could be fitted into two components at 516.2 and 517.3 eV, which can be related to V^{4+} and V^{5+} species, respectively [11, 24]. A greater amount of surface V^{4+} was present on the catalyst calcined at 600 °C than on the catalyst calcined at 500 °C. In addition, the presence of more V^{4+} species in Te-containing samples than Te-free samples, suggested that the presence of Te can favor the reduction of V^{5+}.

The Te 3d5/2 peak of catalysts could be fitted into two components at 576.2 and 577.3 eV, which can be related to Te^{4+} and Te^{6+} species, respectively [11, 25]. It can be seen that only Te^{4+} cations were present on the surface of the $MoV_{0.3}Te_{0.25}O_x$ catalysts.

3.4 H_2-TPR Studies

The H_2-temperature programmed reduction (H_2-TPR) profiles and amount of H_2 consumption of $MoV_{0.3}$-500, $MoV_{0.3}$-600, $MoV_{0.3}Te_{0.25}$-500, and $MoV_{0.3}Te_{0.25}$-600 calcined at 500 °C and 600 °C for 2 h in flowing N_2 are presented in Fig. 4a and Table 2. The TPR profiles of the Te-free samples $MoV_{0.3}$-500 and $MoV_{0.3}$-600 displayed a first TPR peak appeared at about 601 °C or 556 °C, considered to be due to the reduction of the surface-capping oxygen of vanadium and molybdenum, while the main peak at 675 °C or 679 °C, corresponding to the step-wise reduction of $MoO_3 \rightarrow MoO_2$ [11, 26, 27]. In addition, for the Te-doping sample $MoV_{0.3}Te_{0.25}$-500, the H_2-TPR profile also showed two peaks, but the first TPR peak appeared at lower temperature (about 520 °C), indicating the lattice oxygen is more reactive. Similarly, the second TPR peak centered at 676 °C should be ascribed to the reduction of Mo^{6+}. However, the H_2-TPR profile of the Te-doping sample $MoV_{0.3}Te_{0.25}$-600 displays three peaks at 652, 678, and 697 °C. According to previous work [26, 27], the weak reduction peak observed at 652 °C may be attributed to a stepwise reduction of $V_2O_5 \rightarrow 1/3V_6O_{13}$

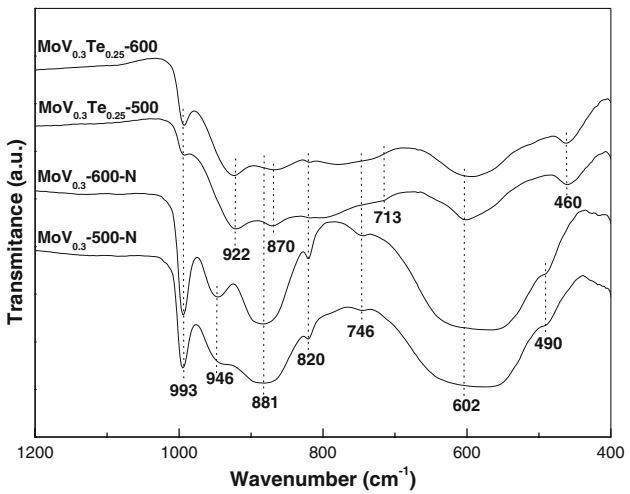

Fig. 2 IR spectra of $MoV_{0.3}O_x$ and $MoV_{0.3}Te_{0.25}O_x$ mixed oxide catalysts calcined at 500 °C and 600 °C for 2 h in flowing N_2

Table 1 BET surface area and XPS data of samples calcined at 500 °C and 600 °C for 2 h in flowing N_2

Sample	S_{BET} (m^2 g^{-1})	Binding energy (eV)				Surface composition (at%)					Surface oxidation states	
		Mo $3d_{5/2}$	V $2p_{3/2}$	Te $3d_{5/2}$	O 1s	Mo	V	Te	O	Te/Mo	Mo^{5+}/Mo^{6+}	V^{4+}/V^{5+}
$MoV_{0.3}$-500	10.5	232.9	516.9	–	530.8	20.2	3.9	–	75.9	–	0.05/0.95	0.01/0.99
$MoV_{0.3}$-600	4.2	232.9	516.9	–	530.8	26.7	3.9	–	69.4	–	0.06/0.94	0.18/0.82
$MoV_{0.3}Te_{0.25}$-500	7.2	232.7	517.8	578.1	531.9	20.8	3.4	4.8	71.0	0.23	0.01/0.99	0.07/0.93
$MoV_{0.3}Te_{0.25}$-600	0.5	232.6	517.7	577.8	531.8	21.4	2.0	4.8	71.8	0.22	0.14/0.86	0.49/0.51

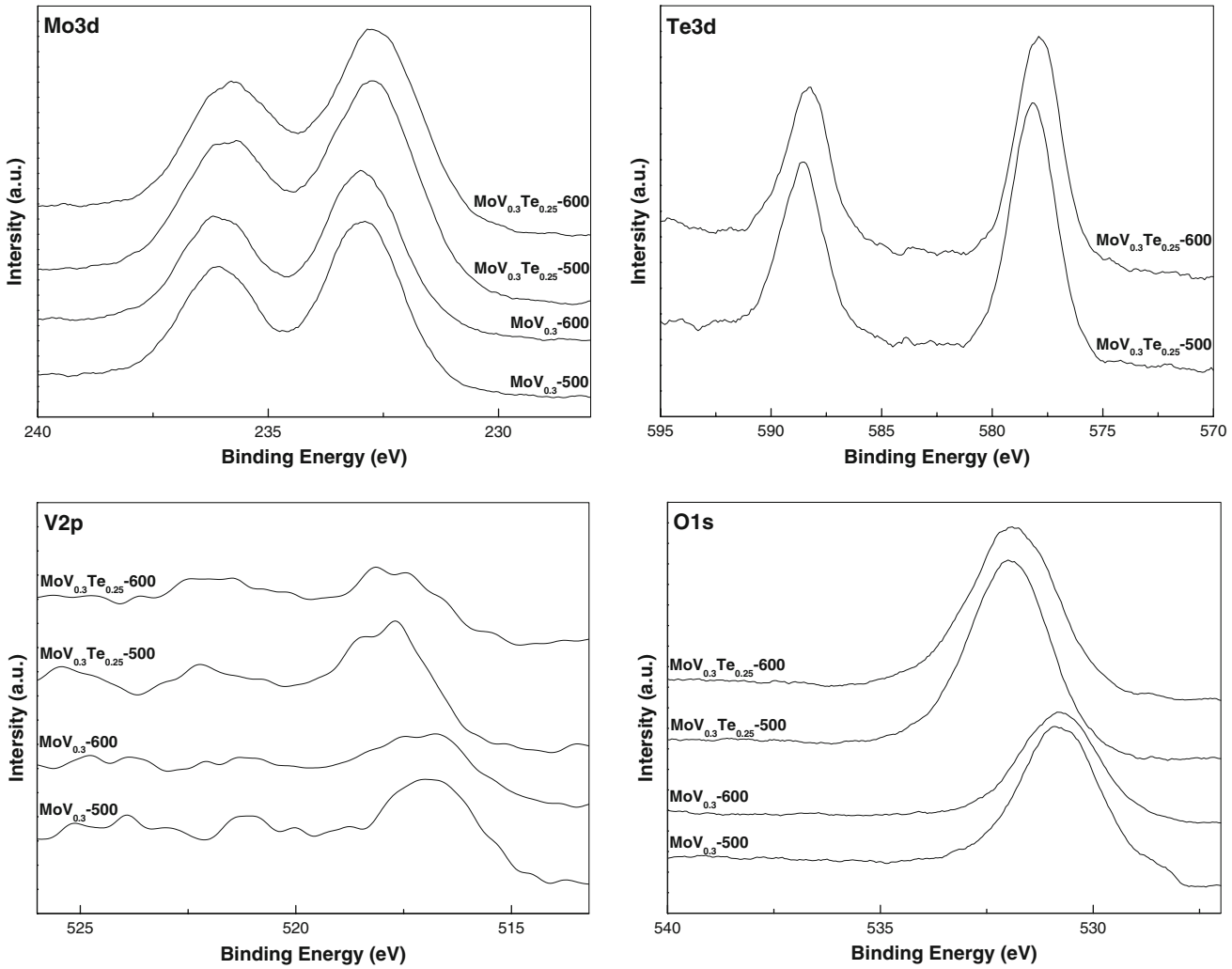

Fig. 3 X-ray photoelectron spectra corresponding to the main transitions (Mo $3d_{5/2}$, Te $3d_{5/2}$, V $2p_{3/2}$, and O 1s) of $MoV_{0.3}O_x$ and $MoV_{0.3}Te_{0.25}O_x$ mixed oxide catalysts calcined at 500 °C and 600 °C for 2 h in flowing N_2

and $TeO_2 \rightarrow Te$. The peak at 678 °C could be related to a stepwise reduction of $MoO_3 \rightarrow MoO_2$, whereas the peak at 697 °C could be assigned to a stepwise reduction of $V_6O_{13} \rightarrow 3VO_2$. In addition, according to the XPS data, relatively high concentration of Mo^{5+} was detected at the surface of $MoV_{0.3}Te_{0.25}$-600 catalyst. These Mo^{5+} species may also contribute to the TPR spectrum, because they began to be reduced when the temperature was above 650 °C [26].

On the other hand, the H_2-TPR profiles of $MoV_{0.3}$-500, $MoV_{0.3}$-600, $MoV_{0.3}Te_{0.25}$-500, and $MoV_{0.3}Te_{0.25}$-600 after the catalytic reaction were also investigated (Fig. 4b). It is apparent that the main TPR peaks of the used catalysts shifted to higher temperatures compared to the fresh ones.

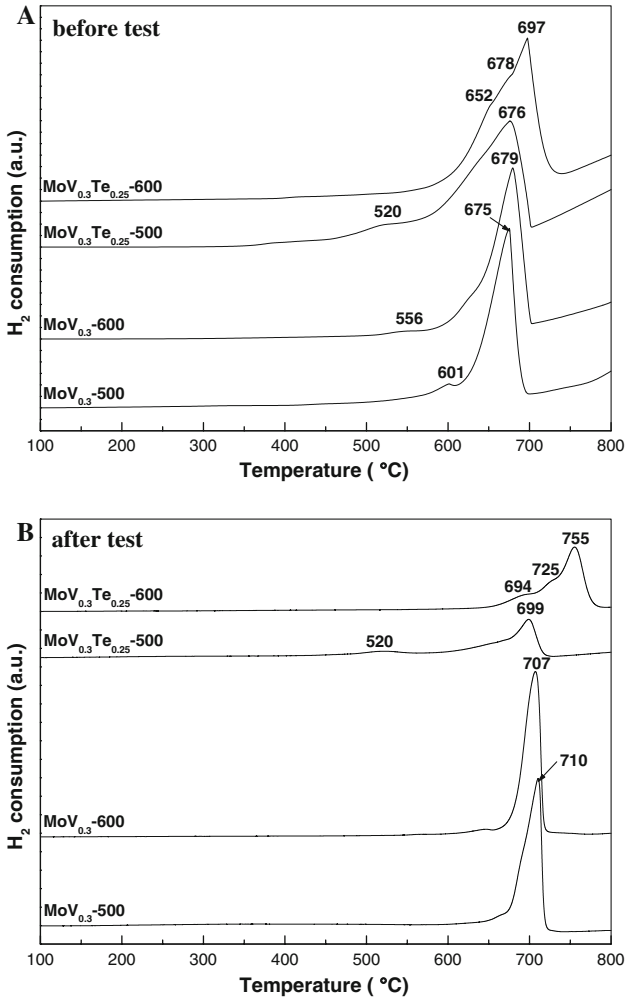

Fig. 4 H_2-TPR profiles of $MoV_{0.3}O_x$ and $MoV_{0.3}Te_{0.25}O_x$ mixed oxide catalysts before and after the catalytic reaction

For the used Te-free catalysts $MoV_{0.3}$-500 and $MoV_{0.3}$-600, the main reduced peak appeared at 710 °C and 707 °C, respectively, which were generally considered to be the reduction of V_6O_{13} [10]. Similar result was presented in the used $MoV_{0.3}Te_{0.25}$-500 catalyst. Furthermore, there are three main reduced peaks in the TPR curve of the used $MoV_{0.3}Te_{0.25}$-600 catalyst, centered at 694, 725, and 755 °C, which should be ascribed to the reduction of V_6O_{13}, Mo^{5+}-species and MoO_2, respectively [10]. It is obvious that there was almost no Mo^{6+} species which was reduced in all of the used catalysts, indicating that Mo^{6+} species in all of the tested catalysts should be involved in the selective O insertion of olefinic intermediate [10].

To estimate the H_2 consumption, the area of TPR profile was integrated with the results shown in Table 2. The H_2 consumption was found to increase in the sequence $MoV_{0.3}$-500 < $MoV_{0.3}$-600 < $MoV_{0.3}Te_{0.25}$-500 < $MoV_{0.3}Te_{0.25}$-600. It is clear that the amount of H_2 consumption of Te-doping samples were larger than those of Te-free samples, which demonstrated that the addition of Te to Mo–V-based system may relatively improve the amount of oxidized species.

3.5 Catalytic Properties

The catalytic results obtained for the oxidation of isobutane over the catalysts at 420 °C, given in Table 3, indicated that the $MoV_{0.3}O_x$ catalysts were active and selective for the partial oxidation of isobutane. However, their selectivity to MAL is very low. The conversion of isobutane and selectivity to MAL was considerably improved by the addition of Te to the system calcined under the same conditions. For example, the selectivity to MAL increased 4.1% for $MoV_{0.3}Te_{0.25}$-500 catalyst and 24.9% for $MoV_{0.3}Te_{0.25}$-600 catalyst in comparison with the corresponding Te-free catalysts. Thereby, it seems that Te may be the favorable element for the activation of isobutane and have a positive effect on the transformation of isobutane to MAL.

In addition, it can be found that the higher selectivity to isobutene and MAL but lower selectivity to MAA was achieved over the catalysts calcined at 600 °C compared with the ones calcined at 500 °C. This observation confirmed the fact that the calcined temperature has evident effect on the catalytic behavior of Mo–V-based catalysts. The catalytic performance of the catalysts calcined at 600 °C was generally better than those calcined at 500 °C.

Considering that the Mo^{5+}/Mo^{6+} surface atomic ratios in the catalysts calcined at 600 °C were higher than those in the catalysts calcined at 500 °C, and the selectivity to MAL over the catalysts calcined at 600 °C was also higher than that over the catalysts calcined at 500 °C, it has been suggested that Mo^{5+} species should be involved in the selective oxidation of isobutane to MAL. However, it is evident that the selectivity to MAL is even higher for $MoV_{0.3}Te_{0.25}$-500 with much lower concentration of Mo^{5+}

Table 2 The H_2-TPR results of samples calcined at 500 °C and 600 °C for 2 h in flowing N_2

	Sample			
	$MoV_{0.3}$-500	$MoV_{0.3}$-600	$MoV_{0.3}Te_{0.25}$-500	$MoV_{0.3}Te_{0.25}$-600
Temperature (°C)	601/675	556/679	520/676	652/678/697
Weight (mg)	10	10	10	10
H_2 consumption (μmol)	1.2/9.2	0.2/10.6	1.5/13.9	10.2/2.8/3.8

Table 3 Catalytic properties of the catalysts for isobutane oxidation at 420 °C[a]

Catalysts	Conversion (%)	Selectivity (%)							
		i-$C_4^=$	MAL	MAA	CO	CO_2	$C_3^=$	ACT	HAC
$MoV_{0.3}$-500	16.1	1.1	8.1	9.0	35.8	28.9	3.0	0.3	13.7
$MoV_{0.3}$-600	13.5	19.8	19.3	3.9	26.2	14.9	6.8	1.1	7.9
$MoV_{0.3}Te_{0.25}$-500	20.1	0	12.2	11.7	31.4	27.7	1.4	0	15.5
$MoV_{0.3}Te_{0.25}$-600	15.6	11.8	44.2	3.5	14.8	10.4	5.7	1.8	7.7

[a] Operating condition: GHSV = 1,800 mL h^{-1} g_{cat}^{-1}, P = 101 kPa

Table 4 Catalytic properties of the catalysts for isobutene oxidation at 420 °C[a]

Catalysts	Conversion (%)	Selectivity (%)						
		MAL	MAA	CO	CO_2	$C_3^=$	ACT	HAC
$MoV_{0.3}$-500	50.3	49.0	2.6	10.0	21.9	0.9	5.1	10.3
$MoV_{0.3}$-600	51.8	26.8	1.9	14.4	31.6	0.9	4.6	19.6
$MoV_{0.3}Te_{0.25}$-500	54.9	22.9	6.3	20.3	37.1	0.9	1.6	10.8
$MoV_{0.3}Te_{0.25}$-600	68.6	64.8	2.9	7.4	15.9	0.6	2.0	6.3

[a] Operating condition: GHSV = 1,800 mL h^{-1} g_{cat}^{-1}, P = 101 kPa

at the surface compared to $MoV_{0.3}$-500. Therefore, it is rational to infer that Te element should be the key factor for the formation of MAL. In other words, the selective oxidation of isobutane to MAL might proceed mainly on the surface of the TeMo-containing crystalline phases (e.g. Mo^{5+}-containing $TeMo_5O_{16}$ phase) [28].

The reaction results of selective oxidation from isobutene to MAL over the catalysts at 420 °C are summarized in Table 4. It can be seen that the selectivity to MAL in the selective oxidation of isobutene over $MoV_{0.3}Te_{0.25}$-600 catalysts is the highest among the four catalysts, which again proves the suggestion that Te-containing Mo^{5+} species favor the formation of MAL. In addition, it can be concluded that the selectivity to MAA in the selective oxidation of isobutane over Mo–V-based catalysts is generally higher than that in the selective oxidation of isobutene. Therefore, it is reasonable to propose that MAA is formed not only from isobutene and MAL, but also directly from isobutane or an intermediate. In other words, MAA is formed following a parallel-consecutive scheme: the consecutive path of the reaction may include the steps: isobutane → isobutene → MAL → MAA → CO_x. The extent of the successive reactions will increase with the increase in total conversion of isobutane.

4 Conclusion

Mo–V–O and Mo–V–Te–O catalysts were obtained by a hydrothermal method. BET surface area showed that the catalysts calcined at high temperature (600 °C) gave lower surface area as compared to those calcined at low temperature (500 °C). Reduction profiles of $MoV_{0.3}Te_{0.25}$-600 catalyst gave reduction peaks associated with Mo^{6+}, Mo^{5+}, V^{5+}, and Te^{4+} species. From the catalytic test for isobutane and isobutene oxidation, $MoV_{0.3}Te_{0.25}$-600 catalyst showed the highest MAL selectivity (44.2%). The TeMo-containing phase was suggested to be active and selective for isobutane and isobutene oxidation.

Acknowledgments This work was supported by the National Basic Research Program of China (2004CB217804) and the National Natural Science Foundation of China (20673046).

References

1. Misono M, Nojiri N (1990) Appl Catal 64:1
2. Mizuno N, Tateishi M, Iwamoto M (1996) J Catal 163:87
3. Mizuno N, Yahiro H (1998) J Phys Chem B 102:437
4. Langpape M, Millet JMM, Ozkan US, Boudeulle M (1999) J Catal 181:80
5. Cavani F, Mezzogori R, Pigamo A, Trifirò F (2003) Top Catal 23:119
6. Brückner A, Scholz G, Heidemann D, Schneider M, Herein D, Bentrup U, Kant M (2007) J Catal 245:369
7. Inoue T, Asakura K, Iwasawa Y (1997) J Catal 171:457
8. Paul JS, Urschey J, Jacobs PA, Maier WF, Verpoort F (2003) J Catal 220:136
9. Guan J, Jia M, Jing S, Wang Z, Xing L, Xu H, Kan Q (2006) Catal Lett 108:125
10. Guan J, Wu S, Jia M, Huang J, Jing S, Xu H, Wang Z, Zhu W, Xing H, Wang H, Kan Q (2007) Catal Commun 8:1219
11. Guan J, Wu S, Wang H, Jing S, Wang G, Zhen K, Kan Q (2007) J Catal 251:354
12. Guan J, Jing S, Wu S, Xu H, Wang Z, Kan Q (2006) React Kinet Catal Lett 90:27
13. Ushikubo T, Oshima K, Kayou A, Vaarkamp M, Hatano M (1997) J Catal 169:394
14. Asakura K, Nakatani K, Kubota T, Iwasawa Y (2000) J Catal 194:309
15. Aouine M, Dubois JL, Millet JMM (2001) Chem Commun 1180
16. Watanabe N, Ueda W (2006) Ind Eng Chem Res 45:607
17. Watanabe H, Koyasu Y (2000) Appl Catal A: Gen 194–195:479
18. Guliants VV, Bhandari R, Swaminathan B, Vasudevan VK, Brongersma HH, Knoester A, Gaffney AM (2005) J Phys Chem B 109:24046

19. Wachs IE (1996) Catal Today 27:437
20. Kuang WX, Fan YN, Yao KW, Che Y (1998) J Solid State Chem 140:354
21. Bart JCJ, Cariati F, Sgamelloti A (1979) Inorg Chim Acta 36:105
22. Zhu Y, Lu W, Li H, Wan H (2007) J Catal 246:382
23. Robinson JW (1974) Handbook of spectroscopy, vol 1. CRC Press, Boca Raton, FL, p 615
24. Demeter M, Newman M, Reichelt W (2000) Surf Sci 454–456:41
25. Hayashi H, Shigemoto N, Sugiyama S, Masaoka N, Saitoh K (1993) Catal Lett 19:273
26. Botto IL, Cabello CI, Thomas HJ (1997) Mater Chem Phys 47:37
27. Chen L, Liang J, Lin H, Weng W, Wan H, Védrine JC (2005) Appl Catal A 293:49
28. Guan J, Xu C, Wang Z, Yang Y, Liu B, Shang F, Shao Y, Kan Q (in press) Catal Lett